

Biomass-Based Composites from Poly(lactic acid) and Wood Flour by Vapor-Phase Assisted Surface Polymerization

Donghee Kim,[†] Yoshito Andou,[‡] Yoshihito Shirai,^{†,‡} and Haruo Nishida^{*,‡}

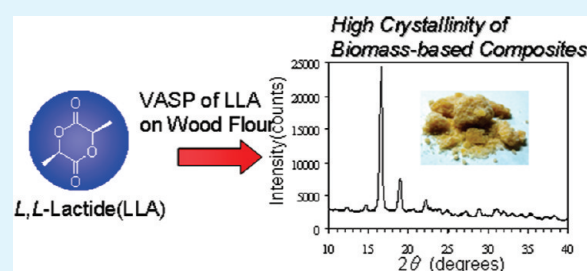
[†]Graduate School of Life Science and Systems Engineering, Kyushu Institute of Technology, 2-4 Hibikino, Wakamatsu-ku, Kitakyushu, Fukuoka 808-0196, and

[‡]Eco-Town Collaborative R&D Center for the Environment and Recycling, Kyushu Institute of Technology, 2-4 Hibikino, Wakamatsu-ku, Kitakyushu, Fukuoka 808-0196, Japan

Supporting Information

ABSTRACT: To prepare biomass-based composites in an environmentally benign manner, vapor-phase assisted surface polymerization (VASP) was applied to prepare the composites from wood flour and poly(L-lactic acid) (PLLA) without solvent. VASP of L,L-lactide successfully proceeded on the wood flour surfaces, resulting in surface coverage by newly generated PLLA. For obtained PLLA/wood flour composites, it was clarified that grafting of PLLA on wood flour surfaces had occurred to form covalently bonded composites, with the accumulated PLLA layers having crystallized in situ during VASP. Resulting PLLA layers showed very high crystallinity of 79.2% and a high melting point close to the equilibrium melting point. Moreover, thermal degradation behavior of the composites suggested a cooperative degradation manner of the components.

KEYWORDS: crystallization, composites, poly(L-lactic acid), vapor-phase assisted surface polymerization, wide-angle X-ray scattering (WAXS)



INTRODUCTION

Lignocellulosic materials such as wood flour, which contain versatile cellulose fibers as a main component, are abundant renewable resources. Many researchers have investigated lignocellulosic composites made up of petroleum-based polymers reinforced by materials, such as jute,^{1,2} coconut,³ sisal,⁴ and kenaf⁵ fibers to develop high-performance materials with a resilience provided by the natural fibers.

Lately, various kinds of bio-based polymeric materials are being developed for use as blend components because of their carbon neutral properties and biodegradability. Poly(L-lactic acid) (PLLA) is one such typical bio-based aliphatic polyester produced from starch, molasses, etc.,⁶ via lactic acid fermentation, oligomerization, cyclic-dimerization, and either ring-opening polymerization of lactide as a cyclic dimer,⁷ or direct polycondensation of lactic acid.^{8–11} PLLA has potential applications to various fields such as medical devices,¹² composite materials,^{13–18} and packages¹⁹ because of its excellent physical properties of transparency, high elastic modulus, and high melting temperature of around 170 °C.²⁰ Composites made from natural fibers and PLLA matrices²¹ have been investigated as promising materials with a low environmental impact when compared with petroleum-based polymer composites. Generally, natural fibers have a large number of hydroxyl and/or carboxyl groups on their surfaces. Thus, when natural fibers are incorporated into commodity plastic matrices, they have been shown to weaken the mechanical properties of the composites

because of the poor interfacial interactions between the hydrophobic plastic matrices and the hydrophilic fibers.²²

Attempts to improve the interfacial adhesion between natural fibers and hydrophobic matrices have been made by the method of surface modification, for example, by using silane cross-linking for wood/PE,^{23–25} esterification-branching/cross-linking for wood/PE/PP²⁶ or wood/PLA,²⁷ etc.

The vapor-phase assisted surface polymerization (VASP) technique, which does not require solvent,^{28–34} has been developed to coat various substrate surfaces with polymers, resulting in the notable achievements of block-copolymer coating, surface grafting, hydrophobic/hydrophilic controlling, and micropatterning. During VASP, vaporized monomers can diffuse and penetrate into the internal gaps and spaces within solid substrates. Even when the gaps are nano-spaces between the silicate layers of montmorillonite, the monomers exfoliate them by in-situ VASP.^{35,36} Thus, VASP is an excellent method for preserving the fine structures of delicate substrate surfaces such as biomaterials, when their chemical properties are being modified. This is because the VASP processes: adsorption of gaseous monomer molecules and simultaneous polymerization, are very gentle in comparison with liquid and melt processes.³⁷ Moreover, there

Received: October 15, 2010

Accepted: December 9, 2010

Published: December 27, 2010

are two additional properties of VASP: the interfacial interaction with substrate surfaces and the formation of highly crystallized polymer layers,²⁹ which open up the possibility for the composite construction of specific surfaces and interfaces having a range of properties at variance with those of previously reported composites prepared by the liquid and melt processes.

In this study, VASP of L,L-lactide was carried out on surfaces of wood flour to produce a biocompatible composite, which was expected to show specific properties based on the simultaneous polymerization/crystallization processes of PLLA at the same point on the surfaces. To clarify the structure and properties of PLLA/wood flour composites, we examined obtained composites using various analytical methods.

EXPERIMENTAL SECTION

Materials. Monomer: L,L-lactide (LLA, 99.6%, melting point 97 °C) was received from Musashino Co., Ltd. (Tokyo, Japan) and purified by two cycles of recrystallization from toluene before use. Substrate: wood flour of Japanese cedar (average diameter: 500 μm) as sawdust was purchased from TRYWOOD Co., Ltd. (Hita, Japan) and used as received. Catalyst, Sn(II) 2-ethylhexanoate (Sn(Oct)₂) was purchased from Wako Pure Chemical Industries, Ltd. (Wako, Japan) and used as received. Commercial poly(L-lactic acid) (PLLA) (TERRAMAC, M_n 42 000, M_w 76 000, L-lactate unit 98.5%) was received from UNITIKA Ltd. and used as a reference material. All the solvents were commercially obtained and used as received.

Typical Procedure of VASP. Substrate: wood flour (2.0 g) was pre-treated with a 0.25 mM CH₂Cl₂ solution of Sn(Oct)₂ (50 mL) at a weight ratio of wood flour:Sn(Oct)₂ = 20:1 (wt %:wt %) at 25 °C for 0.5 h under stirring to adsorb the catalyst on the surface. After the pre-treatment, CH₂Cl₂ was removed under vacuum at 20 °C, resulting in the preparation of a catalyst-supported wood flour substrate.

A typical procedure of VASP was carried out in an H-shaped glass tube reactor with a vacuum cock. The catalyst-supported wood flour (200 mg) was put into a Petri dish (bottom surface area: 116.9 mm²) and the Petri dish set in the bottom of one of the legs of the H-shaped glass tube reactor. Monomer: LLA (2.5g, 17.5 mmol) was introduced into the bottom of the other leg. The reactor was degassed by three freeze–pump–thaw cycles and then sealed under a saturated atmosphere of vaporized LLA. Polymerization was carried out at 110 °C for 24 h in a thermostated oven. At this temperature, LLA melted and evaporated to give a saturated vapor pressure (1.25×10^3 Pa).

After VASP, obtained product was dried to remove adsorbed LLA molecules in vacuo and weighed to yield 1.85 g of the PLLA/wood flour composite. The product was analyzed intact with fourier transform infrared (FTIR) spectroscopy, scanning electron microscopy (SEM), thermogravimetry (TG), differential scanning calorimetry (DSC), and wide-angle X-ray diffractometry (WAXD).

Free-polymers in the PLLA/wood flour composite were extracted by CHCl₃ from the product with a Soxhlet apparatus for 24 h. The isolated polymers were dried and analyzed by FTIR, ¹H-NMR spectroscopy, and size-exclusion chromatography (SEC). The residual wood flour was dried, weighed, and analyzed by FTIR and SEM.

Characterization. ¹H-NMR spectra were measured on a 500 MHz JEOL JNM-ECP500 FT-NMR spectrometer. Chloroform-*d* was used as a solvent and the chemical shifts were reported as δ values (ppm) relative to internal tetramethylsilane (TMS) unless otherwise noted. FTIR spectroscopy was performed using a Perkin Elmer GX2000R FTIR spectrometer equipped with an attenuated total reflectance (ATR) crystal accessory (Golden Gate). SEM observation was performed with a HITACHI S3000N scanning electron microscope at an accelerating voltage of 5.0 kV.

Table 1. Vapor-Phase Assisted Surface Polymerization of L,L-Lactide on Wood Flour Surfaces^a

entry	wood flour ^b			increment		M_n	M_w
	g	catalyst (mmol)	time (h)	g	wt% ^c		
1	0.20	0.025	3	0.16	80.0	300	1,300
2	0.24	0.030	6	0.31	129.2	500	1,600
3	0.22	0.028	9	0.86	390.9	800	2,200
4	0.20	0.025	15	1.25	625.0	1,600	5,100
5	0.25	0.031	24	1.65	660.0	4,700	12,100

^a Conditions: L,L-lactide 17.5 mmol, temperature 110 °C. ^b Sn(II)(Oct)₂ was supported. ^c Against substrate weight.

TG analyses were performed using a SEIKO EXSTAR 6200 TG/DTA system under nitrogen flow (100 mL·min⁻¹) in a temperature range of 30–500 °C. About 6 mg of sample was placed in an aluminum pan and measured. DSC measurements were performed on a SEIKO EXSTAR 6200 DSC system in a nitrogen atmosphere. About 6 mg of the sample was placed on an aluminum pan and a first scan was carried out from room temperature up to 200 °C using a heating rate of 10 °C min⁻¹, followed by cooling to 20 °C at a cooling rate of 10 °C min⁻¹. A second scan was then conducted at the same heating rate in a nitrogen flow of 50 mL min⁻¹.

WAXD patterns were measured on a Rigaku XRD-DSC-X II diffractometer using Cu–Kα radiation ($\lambda = 0.1541$ nm) at room temperature in a 2θ range of 10–40° at a scanning rate of 2 deg·min⁻¹. Molecular weights of polymers were measured on a TOSOH HLC-8120 size exclusion chromatography (SEC) system with refractive index (RI) and ultraviolet (UV, $\lambda = 254$ nm) detectors under the following conditions: TSKgel Super HM-H linear column (linearity range, 1×10^3 to 8×10^6 ; molecular weight exclusion limit, 4×10^6), CHCl₃ (HPLC grade) eluent at a flow rate of 0.6 mL min⁻¹, and column temperature of 40 °C. Calibration curves for SEC analysis were obtained using polystyrene standards with a low polydispersity (7.70×10^2 , 2.43×10^3 , 3.68×10^3 , 1.32×10^4 , 1.87×10^4 , 2.93×10^4 , 4.40×10^4 , 1.14×10^5 , 2.12×10^5 , 3.82×10^5 , 5.61×10^5 , 2.00×10^6 , Aldrich). The sample (15 mg) was dissolved in chloroform (3 mL) and the solution was filtered through a membrane filter with a 0.45 μm pore size. The SEC traces were evaluated by a universal calibration method (UCM) using the published Mark–Houwink–Sakurada constants³⁸ for PLLA and polystyrene at 40 °C as follows:

$$\text{PLLA} : (\eta) = (2.068 \times 10^{-4})M^{0.734}$$

$$\text{Polystyrene} : (\eta) = (2.072 \times 10^{-4})M^{0.655}$$

RESULTS AND DISCUSSION

VASP of LLA on Wood Flour Surfaces. Vapor-phase assisted surface polymerization (VASP) of L,L-lactide (LLA) was carried out on wood flour as a substrate, on which surfaces Sn(II) 2-ethylhexanoate (Sn(Oct)₂) as a well-known catalyst for the anionic ring-opening polymerization of LLA was supported.⁷ The polymerization was conducted under saturated vapor pressure of LLA (1.25×10^3 Pa) at 110 °C as listed in Table 1. Monomer molecules in the gaseous phase were first adsorbed on the surface, after which the adsorbed underwent polymerization. Since the reaction temperature was set at a temperature 13 °C higher than the melting point, 97 °C, of LLA, the adsorbed LLA molecules were able to form a thin layer on the substrate surfaces due to a vapor–liquid equilibrium between the thin layer and the

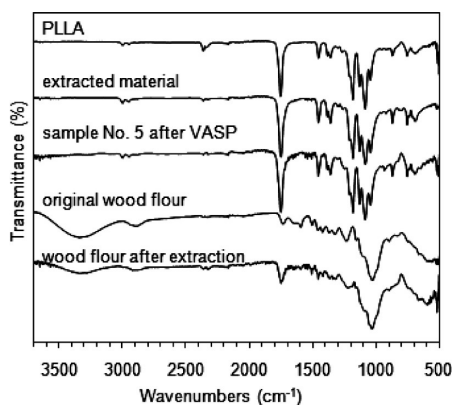


Figure 1. FTIR spectra of original wood flour, sample 5 after VASP of L-lactide, extracted material, residual wood flour after extraction, and PLLA.

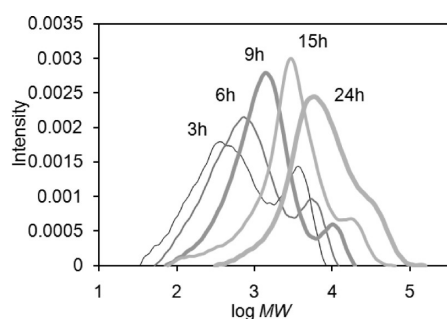


Figure 2. Changes in SEC profile of extracted materials from products after VASP.

saturated vapor phase. Within this thin layer, the LLA molecules may be able to diffuse to active sites on the substrate surface and then undergo polymerization. During VASP, the substrate weight and volume increased in a stepwise fashion with time (Table 1). After 24 h, the product appeared as a lump of aggregated powdery solid (entry 5). On the basis of the increase in weight of the product over a 24 h period, its composition was estimated to be: original wood flour (13.2 wt %) and newly accumulated polymers (86.2 wt %). In Figure 1, the FTIR spectrum of product 5 shows no peak in the wavenumber range of 3100–3700 cm^{-1} corresponding to $\nu_{\text{O-H}}$ of hydroxyl groups in wood flour, indicating that the surfaces were covered by other accumulated materials.

To confirm the properties of the newly accumulated materials on the wood flour surfaces, the products in Table 1 were extracted using CHCl_3 with a Soxhlet extraction apparatus. The FTIR spectrum of the extracted material in Figure 1 shows the same pattern as that of commercial PLLA, exhibiting the characteristic peaks of PLLA at 1760 cm^{-1} assigned to $\nu_{\text{C=O}}$ and 1194, 1130, and 1047 cm^{-1} assigned to $\nu_{\text{C-O}}$.³⁹

Figure 2 shows the changes in SEC profile of the extracted materials from products in Table 1. From the analyses of SEC profiles, the extracted materials were found to be polymeric materials having a molecular weight range of M_w 1300–10 000 with wide polydispersity index (PDI) values in a range of 2.5–4.0. Figure 3 illustrates the ^1H NMR spectra of the extracted materials after 6 and 24 h of VASP (No. 2 and 5 in Table 1) in comparison with commercial PLLA. The observed sharp doublet at 1.57/1.59 ppm and quartet at 5.14–5.20 ppm were assigned to

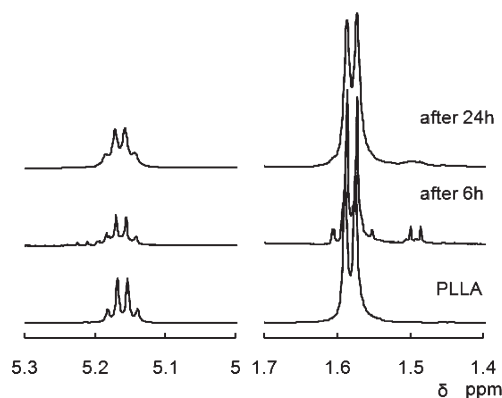


Figure 3. ^1H NMR spectra of PLLA and extracted materials from products after 6 and 24h of VASP.

characteristic signals of $-\text{CH}_3$ and $>\text{CH}-$ in PLLA, respectively. Therefore, these results indicate that the newly accumulated polymeric materials on the wood flour surfaces were PLLA.

All the SEC profiles in Figure 2 exhibited similar multi-modal shapes, reflecting the heterogeneity of the VASP process on the wood flour surfaces in comparison with conventional liquid and bulk polymerization processes.²⁹ The multimodal shape shifted into higher-molecular-weight regions as polymerization progressed. In spite of the heterogeneity of the VASP process, the polymer yield and molecular weight increased in a stepwise fashion with time (Table 1, Figure S1 and S2 in the Supporting Information), with accompanying decreases in PDI value. These results indicate that most polymer chains on the surfaces continue to grow during VASP without any significant termination reactions, suggesting a controlled polymerization manner similar to previous results of VASP using β -propiolactone.²⁹

Changes in Morphology of Wood Flour Surfaces. The substrate wood flour altered its morphology as its volume expanded during VASP. The alteration in the morphology of wood flour was examined by SEM observation. Figure 4 shows SEM images of the wood flour surfaces before (Figure 4a) and after VASP (Figure 4b). Obviously, the wood fibers increased in diameter and their surfaces became flatter after VASP because of being covered by accumulated PLLA layers (see Figure S6 in the Supporting Information). After the extraction treatment by CHCl_3 , the fine structures of the wood flour surfaces were recovered as shown in Figure 4c.

Determination of PLLA-Grafting from Wood Flour Components. In Figure 1, FTIR spectra of composite and extracted PLLA exhibited the same characteristic peaks as commercial PLLA at 1760 cm^{-1} assignable to $\nu_{\text{C=O}}$. However, these carbonyl peaks appeared to be broadened with tailing in comparison with commercial PLLA.⁴⁰ The wood flour components, hemicellulose and lignin, show carbonyl peaks $\nu_{\text{C=O}}$ at 1735 cm^{-1} .^{41,42} In Figure S3 in the Supporting Information, a difference spectrum between the extracted sample 5 and commercial PLLA is illustrated in comparison with original wood flour. Characteristic peaks at 1731 and 1020 cm^{-1} for $\nu_{\text{C=O}}$ and $\nu_{\text{C-O}}$, respectively, suggest the grafting of PLLA on hemicellulose and/or lignin chains.

The $\nu_{\text{C=O}}$ absorption peak on residual wood flour surfaces after the extraction treatment also appeared to be broadened around 1749 cm^{-1} in contrast with the carbonyl peak at 1735 cm^{-1} of original wood flour (Figure 1). After the extraction treatment, the wood flour showed superior water repellency as did the PLLA/wood flour composite in contrast to their original hydrophilic property (see Figure S5 in the Supporting Information).

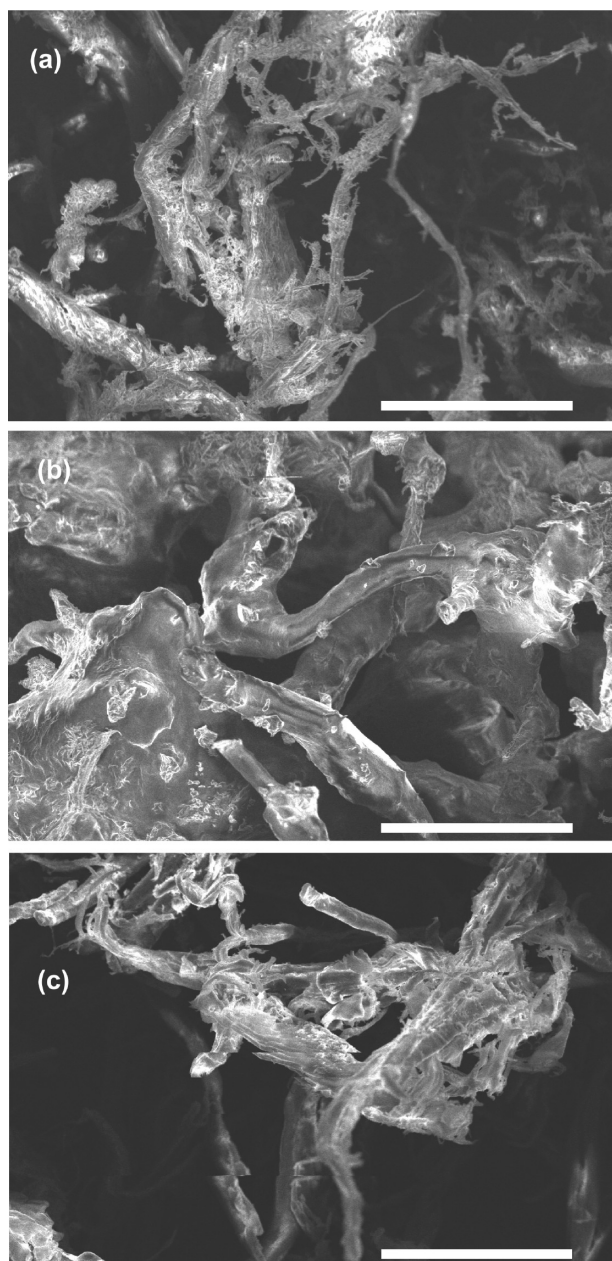


Figure 4. SEM micrographs of (a) original wood flour, (b) sample 5 prepared by VASP of *L,L*-lactide at 110 °C for 24 h, and (c) residual substrates of sample 5 after 24 h extraction using chloroform. Bar: 100 μm .

These characteristics of the wood flour after VASP indicate the grafting of PLLA chains onto the surfaces.

Figure 5 shows changes in the UV/RI intensity ratio of each fraction in SEC profiles of commercial PLLA and the extracted sample 5 after VASP for 24 h. The UV/RI intensity ratio of homopolymer should be nearly constant.²⁸ Commercial PLLA did show a nearly constant plot of UV/RI intensity ratio in a range of 0.03–0.04 over the whole peak profile (Figure 5a). On the other hand, the UV/RI intensity ratio of sample 5 (Figure 5b) increased from 0.03 to 0.6 with increase in molecular weight of product. If polymer chains graft on/from wood flour materials having different UV/RI intensity ratio values, the measured UV/RI ratio value will alter according to the grafting ratio, by which the solubility of graft copolymers in CHCl_3 may also be varied. When

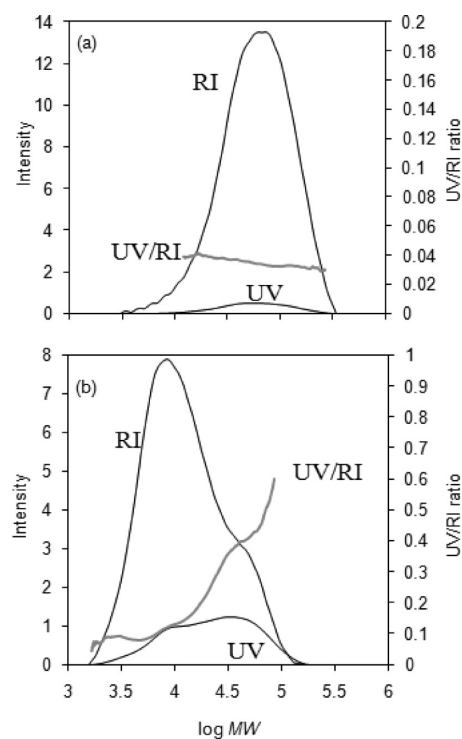


Figure 5. SEC profiles and UV/RI intensity ratios of (a) PLLA and (b) sample 5 after extraction treatment.

the substrate for grafting is a polymeric material, the grafting of PLLA might occur at plural points in the form of increasing branches. Moreover, the grafting causes an increase in total molecular weight. Figure 5b clearly exhibited the increase in the UV/RI ratio value in accordance with the increase in molecular weight. This means that the higher the grafting efficiency, the greater the increase in the molecular weight and UV/RI ratio.

Other samples 1–4 in Table 1 also exhibited similar tendencies in the UV/RI ratio value on their SEC profiles. Moreover, over the whole peak profile, the UV/RI ratio values decreased as the increment of PLLA accumulation increased. This indicates that the tendency of grafting to increase the UV/RI value was being offset by the retarding influence of PLLA accumulation (Table S1 in the Supporting Information).

These results indicate that during VASP some wood flour components were incorporated into the first structures of the accumulated PLLA chains in various covalent bonding manners such as grafting.

Thermal Properties of PLLA/Wood Flour Composites. Thermogravimetric (TG) and differential TG (DTG) profiles of original wood-flour and PLLA/wood-flour composites are shown in Figure 6. All the samples showed multi-step degradation behaviors. Each step corresponds to the degradation of a component. In Figure 6b, many minor DTG peaks appeared at low temperatures. These peaks reflect the heterogeneous initiation and propagation processes of VASP on the wood flour surfaces.³¹

The TG/DTG profiles of original wood flour consisted of two narrow weight loss regions of 250–320 and 320–375 °C for the degradation of hemicellulose and cellulose components, respectively. Moreover, a wide temperature region of 160–900 °C was assigned to the degradation region of lignin ingredient.⁴³ The accumulation of PLLA layers by VASP must newly add more complex degradation steps on the wood flour profiles. Obviously,

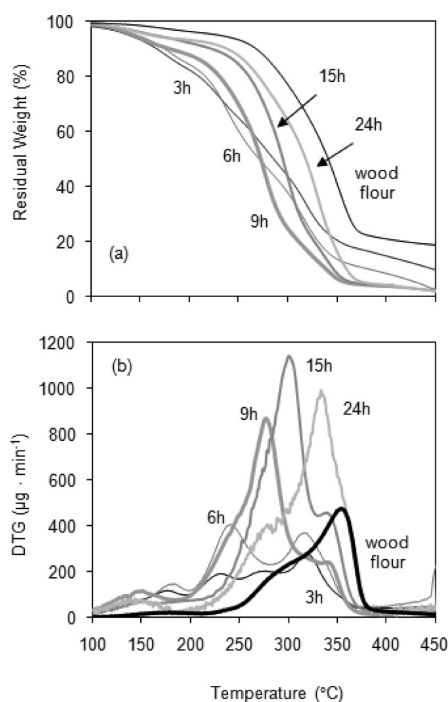


Figure 6. (a) TG and (b) DTG profiles of original wood flour and PLLA/wood flour composites prepared by VASP of LLA.

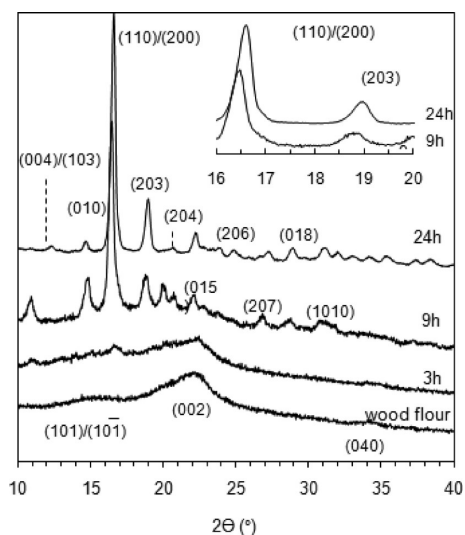


Figure 7. WAXD patterns of samples by VASP of L,L-lactide.

the accumulated PLLA shifts the wood-flour degradation steps towards lower temperature ranges, suggesting an acceleration of wood-flour degradation.

Main DTG peaks of PLLA ingredients clearly appeared as the highest peaks and gradually shifted into higher temperature ranges with increase in increment and molecular weight of the accumulated PLLA. This shift indicates that the higher the molecular weight of accumulated PLLA, the more the composite becomes stable. Moreover, the degradation temperature of the substrate increased to approach that of the original wood flour as the molecular weight of PLLA increased.

Interestingly, when the accumulated PLLA layers were removed by the extraction treatment, the residual wood flour

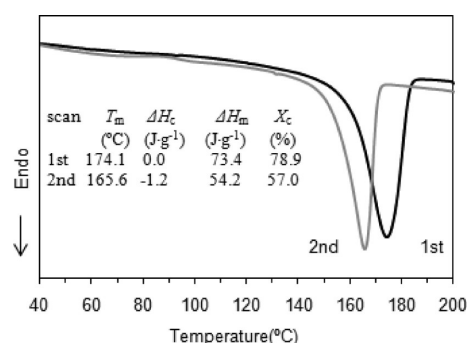


Figure 8. DSC curves of PLLA/wood flour composite (sample 5). Heating and cooling rates are 10°C/min.

ingredient showed nearly the same TG curves as the original wood flour (see Figure S4 in the Supporting Information). These cooperative degradation behaviors of the composites may imply that there are specific interactions at interfaces between the wood flour and the accumulated PLLA layers.

Crystallization Behavior of Accumulated PLLA on Wood Flour Surfaces. In situ crystallization behaviors of accumulated PLLA layers during VASP were analyzed with WAXD. In Figure 7, WAXD profiles of original wood flour and products 1–5 in Table 1 are illustrated. The wood flour profile showed broad diffraction peaks at $2\theta = 14.9, 16.3, 22.5,$ and 34.6° assigned to diffraction planes (101), (10 $\bar{1}$), (002), and (040) of cellulose crystalline, respectively.⁴⁴ With progress in VASP, the diffractions from cellulose crystalline became obscured by the accumulated PLLA layers. After 24 h of VASP, the accumulated PLLA layers were observed to be highly crystallized (79.2%). The WAXD profile of the composite sample after 24 h of VASP showed the typical diffraction pattern of the α -form crystalline of PLLA.^{45,46} The two highest diffraction peaks at $2\theta = 16.6$ and 19.0° correspond to the diffractions from (110)/(200) and (203) planes, respectively.

Interestingly, the WAXD pattern of PLLA layers varied with time of VASP. After 3h, weak diffraction peaks at $2\theta = 11$ and 16.5° were found, and after 9 h other diffraction peaks at $2\theta = 10.9, 14.8$ (010), 16.45 (110)/(200), 18.8 (203), $20.0, 20.7$ (204), 23.7 (015), 26.8 (207), 28.7 (018), and 30.7° (1010) also appeared. As shown at an interposition in Figure 7, significant shifts in the diffraction peak positions from the planes (110)/(200) and (203) were observed from 16.45 to 16.6° and from 18.8 to 19.0° during VASP from 9 to 24 h, respectively. These shifts can be attributed to decreases in lattice d -spacing of the crystalline phase (see Table S2 in the Supporting Information), indicating that the crystalline structure of PLLA transformed from a disordered α' -form to an ordered α -form crystal.^{40,45,46}

The progress in VASP caused not only the disorder-to-order (α' -to- α) transition in PLLA crystalline but also an increase in the crystalline sizes, as shown in Table S2 in the Supporting Information, which were evaluated from the half-width values of diffraction peaks from the planes (110)/(200) and (203).

This α' -to- α transition and very high crystallinity of PLLA crystalline must be due to the polymerization temperature of 110°C . At this temperature, PLLA crystalline undergoes the transition easily,⁴⁰ with low-molecular-weight PLLAs in particular showing high crystal growth rates.⁴⁷ Assignments of newly found diffraction peaks at 10.9 and 20.0° in the profile after VASP for 9 h are now in progress and will be reported elsewhere in the near future.

To confirm the crystallinity value of accumulated PLLA layers, melting point (T_m) and enthalpy change in the melting (ΔH_m)

of PLLA samples just after VASP were measured by DSC. Figure 8 shows first and second scanned DSC curves of PLLA/wood-flour composite (sample 5). At the first scan, the sample showed relatively high $T_m = 174.1\text{ }^\circ\text{C}$ with $\Delta H_c = -0.0\text{ J g}^{-1}$ and $\Delta H_m = 73.4\text{ J g}^{-1}$, where the reduced weight of PLLA layers, calculated from the weight increment value during VASP (Table 1), was employed for the ΔH estimation. At the following second scan, the same sample showed low $T_m = 165.6\text{ }^\circ\text{C}$ with $\Delta H_c = -1.2\text{ J g}^{-1}$ and $\Delta H_m = 54.2\text{ J g}^{-1}$. Crystallinity ($X_c\%$) was evaluated according to the following eq 2⁴⁸

$$X_c\% = 100(\Delta H_c + \Delta H_m)/93 \quad (2)$$

where 93 (J g^{-1}) is the enthalpy of fusion of PLLA crystals having infinite crystal thickness. Obtained $X_c\%$ values were 78.9 and 57.0% for first and second scans. The $X_c\% = 78.9\%$ is nearly equal to the 79.2% estimated from the WAXD profile. Mano et al.⁴⁹ reported that even in the most favorable cases, it is hard to achieve a crystallinity degree in PLLA of above 60%. The high crystallinity of PLLA obtained in this study may be due to some contribution of wood flour surfaces in enhancing the crystallization of accumulated PLLA layers in a manner similar to epitaxial growth. This enhancing effect of the wood flour surfaces was suggested in the DSC cooling process after melt, during which the composite sample showed a crystallization peak at a higher temperature than that of the extracted neat PLLA (see Figure S7 in the Supporting Information).

Pan et al.⁴⁶ reported T_m values of PLLAs having various molecular weights. In their report, a low molecular weight PLLA (M_n 15 400, M_w 21 300) showed $T_m = 160.9\text{ }^\circ\text{C}$ lower than the $173.4\text{ }^\circ\text{C}$ of a high-molecular-weight PLLA (M_n 218 600, M_w 359 200). In this study, in spite of lower molecular weights (M_n 4700, M_w 12 100), sample 5 exhibited a higher $T_m = 174.1\text{ }^\circ\text{C}$ on first scan than the $173.4\text{ }^\circ\text{C}$ of the high-molecular-weight PLLA. Interestingly, the T_m value was nearly the same as the equilibrium T_m^0 ($174.2\text{ }^\circ\text{C}$) of PLLA having M_w 21 300. After melting once, the second scanned DSC curve of sample 5 showed a low $T_m = 165.6\text{ }^\circ\text{C}$ value, even though higher than the $T_m = 160.9\text{ }^\circ\text{C}$ of PLLA having M_w 21 300. This change in T_m value in the second scan may be induced by mixed effects of wood flour surfaces and surrounding melt chains when recrystallized from a melt state after the first scan.

Thus, the PLLA layers accumulated on wood flour surfaces during VASP at $110\text{ }^\circ\text{C}$ were easily crystallized on the surfaces to give T_m values nearly equal to the T_m^0 of PLLA having a similar molecular weight. These results indicate that there are some interactive effects between the wood flour surfaces and PLLA layers, by which the crystallization of accumulated PLLA layers was significantly enhanced.

CONCLUSIONS

Vapor-phase assisted surface polymerization (VASP) was applied to prepare biomass-based composites from wood flour and PLLA. VASP of PLLA successfully proceeded on wood flour surfaces, which became covered by the accumulation of newly generated PLLA. From FTIR and SEC analyses of obtained composites, it was clarified that PLLA chains grafted on/from the wood flour surfaces to form covalently bonded composites. From the thermal degradation behavior of the composites, it was observed that the degradation proceeded in a cooperative manner with the ingredients, such that the degradation behavior of the composites was accelerated by accumulated PLLA. From WAXD and DSC analyses, the accumulated PLLA layers were found to crystallize in situ during VASP at $110\text{ }^\circ\text{C}$, resulting in a very high crystallinity of 79.2% and a high

T_m value close to equilibrium T_m^0 . These results indicate that there are some interactive effects between the wood flour surfaces and PLLA layers.

ASSOCIATED CONTENT

S Supporting Information. Experimental details and additional information (PDF). This material is available free of charge via the Internet at <http://pubs.acs.org>.

AUTHOR INFORMATION

Corresponding Author

*Fax: (+81) 93-695-6233. E-mail: nishida@lisse.kyutech.ac.jp.

REFERENCES

- (1) Chand, N.; Dwivedi, U. K. *Wear* **2006**, *261*, 1057–1063.
- (2) Rana, A. K.; Mandal, A.; Bandyopadhyay, S. *Compos. Sci. Technol.* **2003**, *63*, 801–806.
- (3) Brahmakumar, M.; Pavithran, C.; Pillai, R. M. *Compos. Sci. Technol.* **2005**, *65*, 563–569.
- (4) Sreekumar, P. A.; Joseph, K.; Unnikrishnan, G.; Thomas, S. *Compos. Sci. Technol.* **2007**, *67*, 453–461.
- (5) Zampaloni, M.; Pourboghrat, F.; Yankovich, S. A.; Rodgers, B. N.; Moore, J.; Drzal, L. T.; Mohanty, A. K.; Misra, M. *Composites, Part A* **2007**, *38*, 1569–1580.
- (6) Yin, P. M.; Nishina, N.; Kosakai, Y.; Yahiro, K.; Park, Y.; Okabe, M. *J. Ferment. Bioeng.* **1997**, *84*, 249–253.
- (7) Kricheldorf, H. R.; Kreiser-Saunders, I.; Boettcher, C. *Polymer* **1995**, *36*, 1253–1259.
- (8) Takasu, A.; Narukawa, Y.; Hirabayashi, T. *J. Polym. Sci. Polym. Chem.* **2006**, *44*, 5247–5253.
- (9) Kim, K. W.; Woo, S. I. *Macromol. Chem. Phys.* **2002**, *203*, 2245–2250.
- (10) Achmad, F.; Yamane, K.; Quan, S.; Kokugan, T. *Chem. Eng. J.* **2009**, *151*, 342–350.
- (11) Chen, G.-X.; Kim, H.-S.; Kim, E.-S.; Yoon, J.-S. *Eur. Polym. J.* **2006**, *42*, 468–472.
- (12) Kasuga, T.; Ota, Y.; Nogami, M.; Abe, Y. *Biomaterials* **2001**, *22*, 19–23.
- (13) Huda, M. S.; Drzal, L. T.; Mohanty, A. K.; Misra, M. *Compos. Sci. Technol.* **2006**, *66*, 1813–1824.
- (14) Chen, F.; Liu, L. S.; Cooke, P. H.; Hicks, K. B.; Zhang, J. W. *Ind. Eng. Chem. Res.* **2008**, *47*, 8667–8675.
- (15) Nishino, T.; Hirao, K.; Kotera, M. *Composites, Part A* **2006**, *37*, 2269–2273.
- (16) Wu, T.-M.; Wu, C.-Y. *Polym. Degrad. Stab.* **2006**, *91*, 2198–2204.
- (17) Petersson, L.; Kvien, I.; Oksman, K. *Compos. Sci. Technol.* **2007**, *67*, 2535–2544.
- (18) Noël, M.; Fredon, E.; Mougél, E.; Masson, D.; Masson, E.; Delmotte, L. *Bioresour. Technol.* **2009**, *100*, 4711–4716.
- (19) Lim, L. T.; Auras, R.; Rubino, M. *Prog. Polym. Sci.* **2008**, *33*, 820–852.
- (20) Ajioka, M.; Enomoto, K.; Suzuki, K.; Yamaguchi, A. *J. Environ. Polym. Degrad.* **1995**, *3*, 225–234.
- (21) Tokoro, R.; Vu, D. M.; Okubo, K.; Tanaka, T.; Fujii, T.; Fujiura, T. *J. Mater. Sci.* **2008**, *43*, 775–787.
- (22) Zhang, F. R.; Endo, T.; Qiu, W. L.; Yang, L. Q.; Hirotsu, T. *J. Appl. Polym. Sci.* **2002**, *84*, 1971–1980.
- (23) Grubbstrom, G.; Holmgren, A.; Oksman, K. *Composites, Part A* **2010**, *41*, 678–683.
- (24) Bengtsson, M.; Oksman, K. *Compos. Sci. Technol.* **2006**, *66*, 2177–2186.
- (25) Bengtsson, M.; Oksman, K. *Composites, Part A* **2006**, *37*, 752–765.

- (26) Gao, H.; Song, Y.-m.; Wang, Q.-w.; Han, Z.; Zhang, M.-l. *J. For. Res.* **2008**, *19*, 315–318.
- (27) Wu, C. S. *Polym. Degrad. Stab.* **2009**, *94*, 1076–1084.
- (28) Yasutake, M.; Hiki, S.; Andou, Y.; Nishida, H.; Endo, T. *Macromolecules* **2003**, *36*, 5974–5981.
- (29) Nishida, H.; Yamashita, M.; Andou, Y.; Jeong, J.-M.; Endo, T. *Macromol. Mater. Eng.* **2005**, *290*, 848–856.
- (30) Andou, Y.; Yasutake, M.; Nishida, H.; Endo, T. *J. Photopolym. Sci. Technol.* **2007**, *20*, 523–528.
- (31) Yasutake, M.; Andou, Y.; Hiki, S.; Nishida, H.; Endo, T. *J. Polym. Sci., Part A* **2004**, *42*, 2621–2630.
- (32) Andou, Y.; Yasutake, M.; Jeong, J.-M.; Kaneko, M.; Nishida, H.; Endo, T. *J. Appl. Polym. Sci.* **2007**, *103*, 1879–1886.
- (33) Andou, Y.; Yasutake, M.; Jeong, J.-M.; Nishida, H.; Endo, T. *Macromol. Chem. Phys.* **2005**, *206*, 1778–1783.
- (34) Yasutake, M.; Andou, Y.; Hiki, S.; Nishida, H.; Endo, T. *Macromol. Chem. Phys.* **2004**, *205*, 492–499.
- (35) Andou, Y.; Jeong, J.-M.; Hiki, S.; Nishida, H.; Endo, T. *Macromolecules* **2009**, *42*, 768–772.
- (36) Andou, Y.; Jeong, J.-M.; Nishida, H.; Endo, T. *Macromolecules* **2009**, *42*, 7930–7935.
- (37) Andou, Y.; Jeong, J.-M.; Kaneko, M.; Nishida, H.; Endo, T. *Polym. J.* **2010**, *42*, 519–524.
- (38) Yasuda, N.; Wang, Y.; Tsukegi, T.; Shirai, Y.; Nishida, H. *Polym. Degrad. Stab.* **2010**, *95*, 1238–1243.
- (39) Garlotta, D. *J. Polym. Environ.* **2001**, *9*, 63–84.
- (40) Zhang, J.; Duan, Y.; Sato, H.; Tsuji, H.; Noda, I.; Yan, S.; Ozaki, Y. *Macromolecules* **2005**, *38*, 8012–8021.
- (41) Sgriccia, N.; Hawley, M. C.; Misra, M. *Composites, Part A* **2008**, *39*, 1632–1637.
- (42) Pandey, K. K. *J. Appl. Polym. Sci.* **1999**, *71*, 1969–1975.
- (43) Yang, H.; Yan, R.; Chen, H.; Lee, D. H.; Zheng, C. *Fuel* **2007**, *86*, 1781–1788.
- (44) Wang, K.; Jiang, J. X.; Xu, F.; Sun, R. C. *Polym. Degrad. Stab.* **2009**, *94*, 1379–1388.
- (45) Pan, P.; Zhu, B.; Kai, W.; Dong, T.; Inoue, Y. *Macromolecules* **2008**, *41*, 4296–4304.
- (46) Pan, P.; Kai, W.; Zhu, B.; Dong, T.; Inoue, Y. *Macromolecules* **2007**, *40*, 6898–6905.
- (47) Tsuji, H.; Tezuka, Y.; Saha, S. K.; Suzuki, M.; Itsuno, S. *Polymer* **2005**, *46*, 4917–4927.
- (48) Tsuji, H.; Ikada, Y. *Polymer* **1995**, *36*, 2709–2716.
- (49) Mano, J. F.; Gómez Ribelles, J. L.; Alves, N. M.; Salmerón Sanchez, M. *Polymer* **2005**, *46*, 8258–8265.